Substitution of Cu^{2+} in the Reaction Center Diquinone Electron Acceptor Complex of *Rhodobacter sphaeroides*: Determination of the Metal–Ligand Coordination†

S. K. Buchanan and G. C. Dismukes*
Department of Chemistry, Princeton University, Princeton, New Jersey 08544
Received August 19, 1986; Revised Manuscript Received April 2, 1987

ABSTRACT: The structure of the Fe(II) site in the "ferroquinone" electron acceptor complex of bacterial reaction centers has been studied by using electron paramagnetic resonance (EPR) of reaction centers prepared from *Rhodobacter sphaeroides* cells in which the metal is biosynthetically replaced by Cu(II) during growth. In the dark, a typical Cu(II) spectrum is observable having axial symmetry with $g_{\|} = 2.19$ and $g_{\perp} = 2.05$ and with resolved copper hyperfine peaks ($A_{\|} = 0.0203$ cm^{-1} (199 G); $A_{\perp} = 0.0019$ cm^{-1}). Comparison of the g values and copper hyperfine splittings with those of structurally characterized copper complexes indicates that the ligand geometry in the reaction center is primarily tetragonal with little distortion away from a coplanar set of four nitrogen ligands. All of the peaks of the Cu(II) spectrum show additional ligand hyperfine splitting, arising from coupling to four nitrogen atoms that are indistinguishable [$A_N(\|) = 0.00145$ cm^{-1} (14 G); $A_N(\perp) = 0.0017$ cm^{-1} (18 G)]. This structure is observed at all pH values between 8.0 and 10.0. These nitrogens are likely to be due to four histidine (imidazole) ligands to Cu in the Fe binding site, analogous to the histidine ligands to Fe found in the *Rhodopseudomonas viridis* crystal structure [Deisenhofer, J., Epp, O., Miki, K., Huber, R., & Michel, H. (1985) *Nature (London) 318*, 618]. All of the spectral features were satisfactorily simulated by using an appropriate spin Hamiltonian to extract the spectroscopic factors reported here. This result is in contrast to a recent report [Feher, G., Isaacson, R. A., Debus, R. J., & Okamura, M. Y. (1986) *Biophys. J. 49*, 585a] in which reaction centers were extracted of iron and reconstituted with copper. The EPR spectrum of the copper in this case exhibits greatly reduced hyperfine structure from only three indistinguishable nitrogens, indicating loss or distortion of one imidazole ligand. Furthermore, the substantially reduced copper hyperfine splitting [$A_{\|} = 143$ G (0.0154 cm^{-1}); $A_{\perp}$ = unresolved] indicates that the local symmetry about Cu(II) is significantly reduced from the native tetragonal symmetry for the biosynthetically incorporated Cu(II) site. These changes appear to have little influence on the electron-transfer rate between the primary and secondary quinones which are directly hydrogen bonded to two of the coordinated imidazoles.

Photosynthetic bacterial reaction centers are well-characterized protein–pigment complexes that convert light energy to chemical potential by selective electron and proton transfer. One of the unanswered questions about the mechanism of this process is the role played by the Fe(II) center in the so-called "ferroquinone" electron acceptor complex (Feher & Okamura, 1978). Although the non-heme iron is juxtaposed between the primary and secondary quinone acceptors, no evidence has been reported for oxidation-state changes for the Fe(II) under native conditions that could support a direct redox function. The comparable Fe(II) site in algal and green plant photosystem II reaction center preparations can be oxidized by a variety of oxidants (Petrouleas & Diner, 1986a) or by photoreduction of the primary quinone in the presence of exogenous secondary quinone acceptors (Petrouleas & Diner, 1986b). However, no evidence exists to support this kind of behavior in vivo.

X-ray diffraction studies (to 3-Å resolution) of the *Rhodopseudomonas viridis* reaction center (RC) indicate that the Fe(II) in the ferroquinone complex is coordinated to five protein ligands: four imidazole groups from histidines arranged approximately in a plane and one carboxyl group from glutamic acid occupying an axial position. The two quinone acceptors are in close proximity to two of the imidazole groups, which occupy a trans configuration in the plane; the Fe(II) is thus located midway between Q_A and Q_B (Deisenhofer et al., 1984, 1985; Michel et al., 1986). This arrangement suggests that the metal should influence electron transfer between Q_A and Q_B.

Earlier proposals (Feher & Okamura, 1978) had postulated that the Fe(II) may be directly involved in facilitating electron transfer between the quinones by promoting orbital overlap. In this model, the partially filled orbitals on Fe(II) would serve as the pathway through which the electron is transferred. Experimental evidence supporting the "iron-wire" hypothesis came from magnetic susceptibility (Butler et al., 1980), electron paramagnetic resonance (EPR) spectroscopy (Feher et al., 1972; Dutton et al., 1973; Dismukes et al., 1984; Butler et al., 1984), and Mössbauer spectroscopy (Boso et al., 1981), indicating a weak electronic interaction between Q_A^- and Fe(II), and EPR spectroscopy, indicating an interaction of similar strength between Q_B^- and Fe(II) (Feher & Okamura, 1978; Okamura et al., 1978; Wraight, 1978; Rutherford & Evans, 1979; Dismukes et al., 1984). This interaction established the existence of an orbital pathway for interaction between Q_A and Q_B via the orbitals on Fe(II) (Feher & Okamura, 1978). Evidence disputing the iron-wire hypothesis came from kinetic studies of electron transfer between Q_A^- and Q_B in reaction centers substituted with Mn(II), either by biosynthetic incorporation (Nam et al., 1984) or by extraction of the iron and reconstitution with other transition metals or with no metal (Debus et al., 1986). These studies found essentially unaltered rates of electron transfer or reduction by a factor of only 2 in the metal-free complex. Also, the high proportion of manganese found in place of iron in a wild-type strain of *Rhodobacter sphaeroides* (Agalidis & Reiss-Husson,

†Supported by grants from the Exxon Educational Foundation and the New Jersey Commission on Science and Technology (86-240020-11). G.C.D. acknowledges support from an A. P. Sloan Foundation Award.

0006-2960/87/0426-5049$01.50/0

1983; Rutherford et al., 1985) and the ease with which other divalent ions may be introduced argue against a direct redox function for the metal.

A second proposed role for the Fe(II) has been in stabilizing the one-electron reduction of the primary quinone while destabilizing the two-electron-reduction process that is normally observed with free quinones in aqueous solution and with the secondary quinone acceptor itself within the reaction center complex (Parson & Cogdell, 1975; Dutton et al., 1978; Wraight, 1979; Debus et al., 1986). However, the protein environment of the Q_A site also plays a major role in enhancing the relative stability of the semiquinone Q_A^-, especially the H subunit (Debus et al., 1985a), and in controlling the redox potential of Q_A/Q_A^- (Gunner et al., 1986). Consequently, the individual contributions of the metal and the protein in native reaction centers have not been distinguished by extraction/reconstitution studies, which can influence both.

A third possible role for the metal has been based on the observed reduction in the rate of recombination with the oxidized chlorophyll donor (P^+) formed in the light-induced states $P^+Q_A^-$ and $P^+Q_B^-$ for reaction centers that are frozen under intense illumination compared to dark forzen samples (Ferris et al., 1983; Kleinfeld et al., 1984). This reduction in the rate of recombination was suggested to be due to an increase in the average separation of P^+Q^- (Kleinfeld et al., 1984) or to vibronic trapping of Q^- as an oxygen-centered radical instead of the delocalized anion radical (Ferris et al., 1983). In both interpretations, the local environment around Q gets polarized upon the arrival of the electron; the relative extent to which the protein and the metal are responsible for this is unknown.

A fourth proposal for the role of the metal has been a structural one, serving to hold the subunits of the reaction center together. While it is now established from the diffraction studies on *Rps. viridis* (Deisenhofer et al., 1985) that the four histidine ligands to iron do indeed originate pairwise from the L and M subunits, removal of the metal hardly affects the kinetics of electron transfer between Q_A^- and Q_B (Debus et al., 1985b). Thus the metal cannot be principally responsible for maintaining the structure needed for Q_A and Q_B functioning.

Some clue as to the possible role of the metal has recently come from studies on Fe-extracted reaction centers (Debus et al., 1986). These exhibit a reduced quantum yield at 63% for formation of the charge-separated state $P^+Q_A^-$. This is the clearest influence that the metal has been found to express in the reaction center. The disruptive influence of the metal extraction conditions that are unrelated to the metal environment may be partly or wholly responsible for this small decrease. The lack of a dominant role for the metal ion in the Q_A^- to Q_B electron transfer could mean that a rate-limiting step, such as protonation or a light-induced structural change, must precede electron transfer (Debus et al., 1986).

To further probe the function of the metal site, it is useful to substitute other spectroscopically active transition metals into the ferroquinone complex by biosynthetic substitution. Such studies should enable the use of a wider choice of spectroscopic probes and thus yield information concerning the importance of the identity of the metal ion, its charge density, its valence electron occupancy, and its bonding to ligands, thereby helping to elucidate its enigmatic role in the reaction center. The present study exploits the benefits afforded by using a slowly relaxing spin $S = {}^1/_2$ ion, Cu(II), to probe the metal site by EPR spectroscopy.

Materials and Methods

Cell Growth and Reaction Center Preparation. The R-26.1 carotenoidless mutant of *Rb. sphaeroides* [formerly called *Rhodopseudomonas sphaeroides*; see Imhoff et al. (1984)] will substitute Fe(II) with Mn(II) (~0.6 Mn/RC) (Nam et al., 1983; Feher et al., 1974) and Zn(II) (~0.5 Zn/RC) (Ferris et al., 1983) in growth media that is depleted of Fe and enriched in the alternate metal salt. The wild-type *Rb. sphaeroides* (Y strain) normally incorporates some manganese in place of iron (Agalidis & Reiss-Husson, 1983) and can be induced to incorporate up to ~90% Mn(II) (Rutherford et al., 1985). Furthermore, the metal can be replaced almost completely by Cu(II) in wild-type *Rb. sphaeroides* (strain Y) when grown on iron-depleted, copper-enriched media, as shown here. This biosynthetic method allows for the study of the metal-substituted bacteria in their native environment.

Rb. sphaeroides wild-type (Y strain) were grown phototropically as described by Reed and Clayton (1968). Cultures were the kind gift of Dr. F. Reiss-Husson, CNRS, Gif-sur-Yvette, France. Cu-enriched cells were grown on Hutner's medium containing no yeast extract, 2.7×10^{-4} M $CuSO_4 \cdot 5H_2O$ and 7.2×10^{-8} M $FeSO_4 \cdot 7H_2O$. All chemicals were of reagent grade except where analytical grades were available. All solutions were prepared with deionized water having undetectable amounts of Fe and Cu as determined by atomic absorption. An aliquot of 0.5 mL of packed normal cells was used to start a single 250-mL culture (modified media) which when mature, was used to inoculate 2-L bottles. Subsequent inoculations were made by using cells from Cu-enriched cultures to further reduce the original Fe and Mn contents.

Reaction centers were isolated from late log-phase cells as described by Reiss-Husson (Jolchine & Reiss-Husson, 1974). This procedure differs from the R-26 methodology (Feher & Okamura, 1978) in the temperature requirements for detergent treatment and ammonium sulfate fractionation and in the required detergent concentration. The final reaction center preparation was further purified by fast-protein liquid chromatography (Pharmacia) using a Mono-Q column with gradient elution. This yielded preparations having an absorbance ratio of $A(280\text{ nm})/A(800\text{ nm}) = 1.3$–$1.6$. The absence of the LHC2 complex was confirmed by sodium dodecyl sulfate gel electrophoresis and by the complete photobleaching of the P865 band.

Final reaction center concentrations were typically 200–250 μM in 10 mM tris(hydroxymethyl)aminoethane buffer (pH 7.8) with 0.1% lauryldimethylamine oxide (LDAO) for EPR measurements. The amounts of copper and iron bound to these preparations were measured by flameless atomic absorption as in the paper by Nam et al. (1984).

EPR measurements were carried out at X-band (~9.1 GHz), as previously described (Dismukes & Siderer, 1981). A 300-W projector lamp was used to illuminate samples at room temperature with subsequent freezing in dry ice/methanol.

To enhance the light-induced signal due to $Cu^{2+}O_A^-$, samples were frozen under illumination in the presence of cytochrome *c* (horse heart; United States Biochemicals) and ascorbate. This eliminates the $g = 2.0026$ signal due to the photooxidized primary donor and ensures maximum reduction of the quinones.

Results

Determination of Cu and Fe. Quantitative analysis of the Cu and Fe contents of the Cu-enriched reaction centers (Table I) shows that 85% replacement of Fe by Cu occurs and that the total Fe + Cu content equals 1.10 per RC.

Cu(II) EPR. Figure 1 illustrates the unexpectedly high resolution observable in the EPR spectrum of the Cu(II) site

Table I: Atomic Absorption Data for Fe and Cu Reaction Centers from *Rb. sphaeroides* Grown in Normal and Cu-Enriched Media

resonance line (Å) (element)	rel sensitivity[a] (μg/mL)	normal Fe media		Cu-enriched media	
		Fe/RC	Cu/RC	Fe/RC	Cu/RC
2483 (Fe)	0.045	1.00 ± 0.02		0.25 ± 0.1[b]	
3247 (Cu)	0.063		<0.02		0.85 ± 0.1[b]

[a] Concentration giving 1% absorption. [b] The value given here refers to the range of metal content from several preparations rather than the single measurement, which is 0.02.

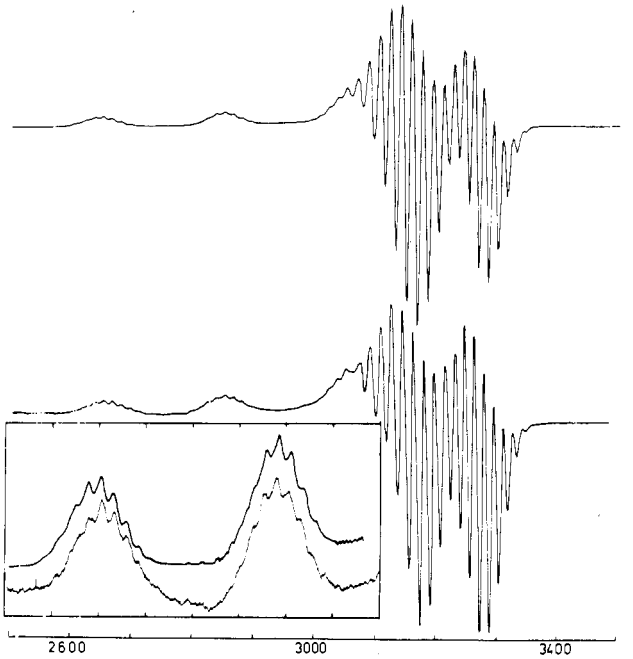

FIGURE 1: EPR spectrum from copper-containing reaction centers, recorded in the dark at 85 K. EPR spectrometer settings were microwave frequency 9.05 GHz, microwave power 5 mW, modulation amplitude 6.3 G, modulation frequency 100 kHz. Reaction center concentration, 250 μM with 0.1% LDAO. (Insert) Expansion of the $M_I = -3/2$ and $M_I = -1/2$ peaks. Bottom trace, experimental; top trace, calculated. Parameters for the simulation are $g_\parallel = 2.19$; $g_\perp = 2.05$; $A_\perp = 0.0203$ cm^{-1}; $A_\perp = 0.0019$ cm^{-1} (^{63}Cu × 1.07 for ^{65}Cu, weight = 0.45); $A_x(N) = 0.00145$ cm^{-1}; $A_{x,y}(N) = 0.0017$ cm^{-1}; line width = 6.5.

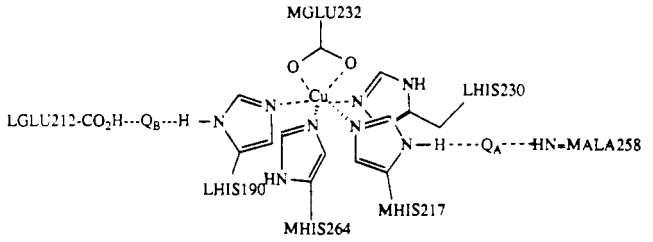

FIGURE 2: Postulated copper diquinone structure in biosynthetically incorporated copper reaction centers. The Cu(II) is coordinated to four histidine residues (two each from the L and M subunits) and to one glutamic acid acting as a bidentate ligand by analogy with the Fe site in *Rb. viridis* (Michel et al., 1986).

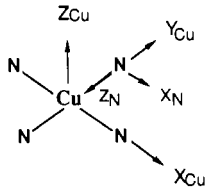

FIGURE 3: Axis system used to define the copper hyperfine and nitrogen hyperfine tensors for the computed spectra.

in dark-adapted reaction centers at 85 K. Readily identifiable features such as g anisotropy ($g_\parallel - g_\perp$), copper hyperfine anisotropy ($A_\parallel - A_\perp$), and ligand superhyperfine structure (A_N), serve to characterize the symmetry of the Cu(II) site and to identify nitrogens as ligands to copper. The occurrence of highly resolved nitrogen couplings on both the $g_\parallel$ and $g_\perp$ regions is not commonly observable in copper proteins. It occurs in cases where there is minimal g and A strain, such as in copper complexes having little structural disorder (Rakbit et al., 1985). This indicates that the metal site in biosynthetically copper substituted reaction centers exhibits a high degree of structural homogeneity.

The g tensor is nearly axially symmetric with $g_\parallel = 2.19$ and $g_\perp = 2.05$, indicative of tetragonally elongated symmetry for the coordinated ligands. Because $g_\parallel > g_\perp > 2.0$, the unpaired electron in the d^9 configuration is in the $d_{x^2-y^2}$ orbital which lies in the tetragonal plane directed at the nitrogen ligands (Figure 2) (Hathaway & Billing, 1970).

For sites oriented in the magnetic field so that the tetragonal axis lies parallel to the field, three of the four possible copper hyperfine peaks are resolved with a splitting of 200 G for the low-field pair of lines. These are attributed to the $M_I = -3/2$, $-1/2$, and $+1/2$ transition on the basis of the good agreement observed with a computer simulation using a spin Hamiltonian appropriate for Cu(II) (vide infra). The spectroscopically derived value for $A_\parallel$ from this simulation is 0.0203 cm^{-1} (199 G). The computed spectrum is shown above the experimental spectrum in Figure 1.

The most conspicuous feature of the spectrum is a pattern of ligand hyperfine lines superimposed on each of the Cu hyperfine peaks, which is characteristic of coupling to nitrogen nuclei (^{14}N, $I = 1$). This pattern is seen readily in the high-field region in Figure 1, where the average splitting is 16.5 G. The large doublet splitting of nine lines each cannot be directly assigned to a fundamental splitting since this structure arises from both the hyperfine structure of the copper ($A_\perp$) and nitrogen ligands, as well as from the angular anomaly in the $g_\perp$ region (Boas et al., 1978). A simpler pattern is seen on the two low-field M_I components of $g_\parallel$, as shown more clearly in the inset to Figure 1, where the average splitting is 14.3 G. Satisfactory fits to these experimental spectra were obtained by computer simulation only when four nitrogen ligands and the natural abundance distribution of the two magnetic copper isotopes were included (vide infra). For this simulation the nitrogen hyperfine interactions were assumed to be axially symmetric with coincident tensors for all N ligands. For convenience in the calculations these were expressed in the same axis system as the Cu hyperfine tensor, given in Figure 3. The nitrogen hyperfine couplings within this axis system are designated $A_z(N)$ and $A_x(N) = A_y(N)$. These may be converted to the local axis system of the nitrogen hyperfine interaction, for which the Cu–N bond axis is the natural axis system. The nitrogen hyperfine components perpendicular and parallel to the Cu–N bond vector are then $A_N(\perp) = A_z(N)$ and $A_{x,y}(N) = 0.5[A_N(\parallel) + A_N(\perp)]$. Inclusion of small inequivalencies in the hyperfine constants for the four nitrogens could not be resolved in the simulated spectra.

The samples contain copper in natural abundance (^{63}Cu, 69.1%; ^{65}Cu, 30.1%), so two magnetic isotopes contribute to

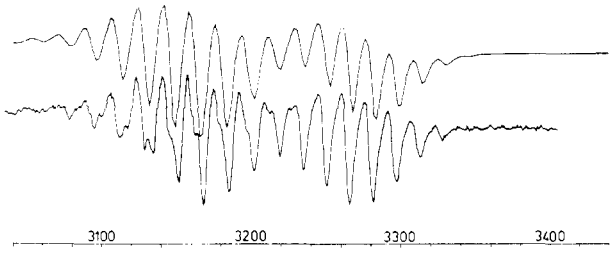

FIGURE 4: Expansion of the $g_\perp$ and angular anomaly regions showing the ^{14}N and $^{63,65}Cu$ hyperfine structure. Bottom trace, experimental; top trace, calculated. Refer to Figure 1 for parameters.

the spectrum. The difference in their magnetic moments is only 6.6% (Weast, 1982), and both have nuclear spins with $I = {}^3/_2$, so they will be difficult to resolve. For this reason it is unwise to interpret the number of nitrogen ligands simply from the number of lines without analysis by simulation. From the known difference in the magnetic moments for these isotopes and the observed values for $A_\parallel$ and $A_\perp$, the predicted separation of the lines between the less abundant ^{65}Cu transitions and those for the ^{63}Cu ought to be 2 G for $M_I = -{}^3/_2$ and $+{}^3/_2$ on $g_\parallel$, 7 G for $M_I = {}^1/_2$ on $g_\perp$, and $g_\perp$, and 21 G for $M_I = {}^3/_2$ on $g_\parallel$. While no resolved structure of this type could be identified on the two low-field Cu peaks, inclusion of both Cu isotopes in the simulations was essential to obtain the quality of fits shown in Figures 1 and 4. A weak splitting of the nitrogen hyperfine peaks by 3–4 G can be seen on some peaks in the $g_\perp$ region (Figure 4). The origin of these satellite peaks is not understood. These peaks were not predicted by the calculations, suggesting that they may be features arising from the anticipated magnetic inequivalence of N ligands whose Cu–N vectors lie parallel and perpendicular to the external magnetic field oriented along $g_\perp$. This is a limitation of the calculation. The possibility of these peaks being due to forbidden nitrogen hyperfine transitions arising from the nuclear electric quadrupolar coupling was not considered quantitatively in the simulations and may possibly contribute to this structure.

The dipolar contribution to the nitrogen hyperfine splitting $\mathcal{D}$ can be estimated from the difference of $A_N(\parallel)$ and $A_N(\perp)$:

$$|A_N(\parallel) - A_N(\perp)| = \mathcal{D}[3(g^2_\parallel/g^2)\cos^2\theta - 1] \quad (1)$$
$$\theta = 0 \text{ and } \pi/2$$

This value of $|A_N(\parallel) - A_N(\perp)|$ from the simulation of the spectra in Figures 1 and 3 was 0.0005 cm^{-1} (4.0 G). This can be compared with the experimentally observed 3–4-G splitting in the $g_\perp$ region thought to be due to this same difference (Figure 3). By use of this as a range of acceptable values for $A_N(\parallel)$ and $A_N(\perp)$, with $g_\perp = 2.19$ and $g = 2.10$, the dipolar splitting term is $\mathcal{D} = (10.1 \pm 3) \times 10^{-5}$ cm^{-1}. An estimate of the Cu–N bond distance can be made through its relationship with the magnitude of the N dipolar hyperfine coupling in

$$R_{Cu-N} = [(g_N\beta_N g\beta_e)/\mathcal{D}]^{1/3} \quad (2)$$

With $g_N = 0.403$ for ^{14}N (Weast, 1982), the resulting distance is 135 pm. This estimate is a lower limit for the Cu–N distance because it is based upon the assumption that all of the spin is localized at the Cu nucleus.

Cu(II) EPR pH Dependence. Copper hyperfine coupling constants and nitrogen hyperfine coupling constants were studied at pH 8.0, 8.5, 9.0, 9.5, and 10.0 and were found to be invariant over this range.

Cu(II)Q^- EPR. Spectral changes are observable at low temperature (10 K) upon light adaptation in the presence of ascorbate and cytochrome *c*. These appear to be related to photoreduction of Q_A. A systematic study of these changes will be conducted and reported in the future.

A photoinducible free radical signal at $g = 2.00$ with line width $\Delta H = 9.8$ G attributable to P865(+) is observed in preparations that are light adapted in the absence of ascorbate and cytochrome *c*. The amplitude of this signal, normalized to total BChl, is not distinguishable in normal Fe vs. Cu-enriched centers. This indicates that RCs substituted with copper are photoactive; the observed activity is not due solely to a small residual iron population in the samples.

Calculated EPR Spectra. The experimental Cu(II) EPR spectra were compared to computed spectra in order to extract the effective spin Hamiltonian parameters describing the fundamental interactions. The computed spectra given in Figures 1 and 4 were derived from a spin Hamiltonian that included anisotropic *g* and Cu hyperfine tensors having collinear orientations. Anisotropic ligand hyperfine coupling to four indistinguishable nitrogen atoms was also included. A second Cu isotope was included in which the coupling constant was 1.07 times that for the first isotope and had a weight of 0.45 times that for the first isotope to account for both ^{63}Cu and ^{65}Cu. The simulations given in Figures 1 and 4 were performed by Drs. Sandra Eaton (University of Colorado, Denver) and Gareth Eaton (University of Denver), using a program called MONMER. This program uses a second-order perturbation treatment including the dependence of transition probability on $1/g$. It does not treat quadrupole interactions. The equations used in this treatment are based on those presented by Toy et al. (1971) and Pilbrow (1969). The spin Hamiltonian parameters used to simulate the experimental spectra are given in the figure legends and summarized in Table II.

DISCUSSION

When compared to the $A_\parallel$ values observed for a number of structurally characterized Cu(II) complexes having nitrogen ligands, as given in Table II and by Hathaway and Billing (1970), the large Cu hyperfine coupling found for the reaction center site ($A_\parallel = 200$ G, low-field splitting; 0.0203 cm^{-1} from the simulation) agrees well with that found in complexes of tetragonal symmetry (octahedral, square planar, or square pyramidal) rather than tetrahedral. For the Cu complexes having different ligand types, there are differences in the magnitude of this coupling that reflect covalency differences of the ligands rather than orbital mixing differences brought about by the symmetry of the ligand field. However, Table II shows clearly that, for complexes having the same ligand type, but with increasing dihedral angle of the four ligands ($\alpha = 0$ for square planar), there is a large, parallel reduction in the value of $A_\parallel$. Because the dipolar hyperfine contribution is positive while the isotropic Fermi contact contribution is negative, this reduction has been attributed to a greater admixture of Cu 4s orbital contribution into the orbital carrying the unpaired electron in symmetries lower than tetragonal (Symons, 1978). We estimate the departure from a coplanar array of four nitrogen atoms to be less than $\alpha = 15°$, on the basis of a comparison of the $g_\parallel$ and $A_\parallel$ values with the values observed for $^{65}Cu(ImH)_4HPO_4$ in frozen aqueous solutions (Table II). This is known from X-ray diffraction studies of the diiodide and the sulfate analogues to be essentially square planar in the solid state (Aktar et al., 1968; Fransson & Lundberg, 1972).

The correlation between α and both *g* and *A* is also illustrated by the Cu(II) tropocoronands given in Table II (Davis et al., 1985). In this series, there is a smoothly varying dis-

Table II: Experimental EPR Parameters for Copper Complexes

complex	abbrev	$g_\parallel$	$g_\perp$	$A_\parallel$	A_N[a]	geom[b]	dihedral angle, α[c]	ref[d]
copper(II) tropocoronand, $CuC_{20}H_{22}N_4$	Cu(TC-3,3)	2.147	2.075	217.5G	14.5[e]	D_{4h}	0.0	1
copper(II) tropocoronand, $CuC_{22}H_{26}N_4$	Cu(TC-4,4)	2.155	2.083	188		↓	36.3	1
copper(II) tropocoronand, $CuC_{24}H_{30}N_4$	Cu(TC-5,5)	2.219	2.062	142		T_d	61.3	1
bis(*N*-methylsalicylaldiminato)copper(II)	$Cu(msaln)_2$	2.225	2.053	171.6		D_{4h}	~0	2
bis(*N*-ethylsalicylaldiminato)copper (II)	$Cu(esaln)_2$	2.220	2.060	161.1				2
bis(*N*-propylsalicylaldiminato)copper(II)	$Cu(psaln)_2$	2.229	2.067	164.9		↓	↓	2
bis(*N*-*tert*-butylsalicylaldiminato)copper(II)	$Cu(bsaln)_2$	2.273		119.3		T_d	~90	2
bis(glycinato)copper(II)	$Cu(gly)_2$	2.232	2.065	152.1		D_{4h}	~0	2
bi(*N*,*N*-dimethylglycinato)copper(II)	$Cu(dmgly)_2$	2.217	2.067	157.7	10.4			2
bis(*N*,*N*-diethylglycinato)copper(II)	$Cu(degly)_2$	2.220	2.060	161.3	9.3			2
bis(*N*,*N*-di-*n*-propylglycinato)copper(II)	$Cu(dpgly)_2$	2.219	2.057	163.2	7.4	O_h	~0	2
copper(II) dimethylglyoxime	$Cu(HD)_2$	2.176	2.053	196	15.6	D_{4h}	0	3
$^{65}Cu(ImH)_4HPO_4$		2.255	2.0	196	14.2	D_{4h}	0	4
Rb. sphaeroides, extracted of Fe and reconstituted with $^{65}Cu(II)$; R-26.1 carotenoidless mutant	CuRC, R-26	2.31	2.07	143	10.9	unknown		5
Rb. sphaeroides, biosynthetic Cu(II) incorporation; wild-type strain Y	CuRC, WT	2.19	2.05	199	16.0	tetragonal		this work[f]

[a] $A_N = \{[A_N(\parallel) + 2A_N(\perp)]/3\}$. For some complexes $A_N(\perp)$ was not resolved. [b] D_{4h}, square planar; O_h, octahedral; T_d, tetrahedral. [c] α is defined as the dihedral angle between the two CuN_2 planes. [d] References are (1) Davis et al. (1985), (2) Nonaka et al. (1974), (3) Falk et al. (1970), (4) Van Camp et al. (1981), and (5) Feher et al. (1986). [e] W. M. Davis and S. J. Lippard, communication. [f] Taken from the best fit computed spectrum with $A_\parallel = 0.0203\ cm^{-1}$, $A_\perp = 0.0019\ cm^{-1}$ (^{63}Cu and X1.07 for the second isotope ^{65}Cu), $A_N(\parallel) = 20.4 \times 10^{-4}\ cm^{-1}$, and $A_N(\perp) = 14.5 \times 10^{-4}\ cm^{-1}$.

tortion of the copper center: Cu(TC-3,3), $\alpha = 0$, $A_\parallel = 217.5$ G; Cu(TC-4,4), $\alpha = 36.3$, $A_\parallel = 188$ G; and Cu(TC-5,5), $\alpha = 61.3$, $A_\parallel = 142$ G. Using the ^{14}N isotropic hyperfine values to gauge the degree of ligand covalency appropriate to imidazole ligands, we see that the value of copper A indicates a nearly square-planar geometry for the Cu site in reaction centers.

The difference in the parallel vs. perpendicular nitrogen hyperfine splittings for ligands coordinated to square-planar Cu(II) complexes, $A_N(\parallel) - A_N(\perp)$, is well understood to be due to the dipolar contribution to the hyperfine interactions (Symons, 1978; Rist & Hyde, 1970). The lower limit estimate for the Cu–N distance of 135 pm based on this dipolar part can be compared with the average Cu–N distance of 200 pm observed in the tetragonal complex $Cu(ImH)_4I_2$ (Aktar et al., 1968) and 201 pm in $Cu(ImH)_4SO_4$ by X-ray diffraction (Fransson & Lundberg, 1972). The Fe–N distances in the *Rps. viridis* reaction center have not been reported yet but will probably emerge as the structure continues to be refined (Michel et al., 1986).

Despite the large difference in the valence electron occupancy of the metals that successfully function in the ferroquinone site (Mn, Fe, Co, Ni, Cu, and Zn), in both metal-reconstituted reaction centers (Debus et al., 1986) and in biosynthetically grown cells (Nam et al., 1984; Buchanan and Dismukes, unpublished results), there is no strong preference for metal type. This argues strongly against a redox function for the metal. There is no evidence that reaction centers which have no metal in the ferroquinone site exist, except for metal-extracted samples. It is not known presently if the metal site becomes protonated in such samples or whether this might account for the relatively minor consequences that metal extraction has on the kinetics of electron transfer from Q_A^- to Q_B or on the lifetime of $P^+Q_A^-$.

The EPR parameters observed for the ^{65}Cu site in reaction centers of the R-26.1 mutant of *Rb. sphaeroides* obtained by extraction of iron and reconstitution with copper (Debus et al., 1986) are very different from those obtained in this study by using biosynthetic incorporation. These differences, which are summarized in Table II, indicate a large increase in $g_\parallel$ from 2.19 to 2.31, a reduction in $A_\parallel$ from 200 to 143 G (low-field splitting), a complete loss of resolvable ^{14}N hyperfine structure on $g_\perp$, a decrease in the ^{14}N hyperfine splitting from 14.3 to 10.9 G on $g_\parallel$, and a reduction in the number of ^{14}N peaks from nine to seven (loss of one N ligand). The structure of the metal site in biosynthetically incorporated Cu reaction centers of *Rb. sphaeroides* strain Y exhibits greater homogeneity, higher symmetry, and coordination of all four nitrogen ligands, while that obtained by reconsitution of Cu(II) to iron-extracted reaction centers of the R-26 carotenoidless mutant (strain 2.4.1) contains only three coordinated nitrogen ligands that are detectable. The quantum yield for formation of $P^+Q_A^-$ is 100% of the control yield (Fe-containing cells) in the former preparation while only 63% in the reconstituted preparation (Debus et al., 1986). The electron-transfer rate from Q_A^- to Q_B is essentially unaltered in these reconstituted preparations. While this rate has not yet been determined for the biosynthetically incorporated Cu reaction centers, for Mn (Nam et al., 1984) and Zn (Ferris, Eckart, and Dismukes, unpublished results) the rate is the same as for the Fe reaction centers. Three explanations seem possible to account for this: (1) the structure of the metal site has no influence on the functioning of the ferroquinone complex, (2) there is a significant difference between the two strains, or (3) the Cu-reconstituted reaction centers form a structurally altered site when reconstituted in the dark (with only three imidazoles coordinated to Cu), but this relaxes to the four coordinated tetragonal form following light-induced turnover. The latter possibility would provide a satisfying explanation of the similar kinetics and quantum yield but has not yet been investigated.

Conclusions

From the correlation of EPR parameters for copper-substituted RCs with known copper complexes, the environment of the Cu(II) ion must involve four EPR indistinguishable N-donor ligands, presumably from the N_ϵ atoms of imidazoles (histidine) in an essentially tetragonal arrangement. This finding is consistent with the X-ray diffraction structure in *Rps. viridis* showing a distorted octahedral coordination for Fe(II) with the N_ϵ from four histidines (roughly tetragonal) and a (possibly) bidentate carboxylate from glutamic acid (Michel et al., 1986). The limited structural information published from the diffraction studies does not permit a closer comparison. Once this is available, it will be interesting to examine whether the different electronic structures of Cu(II) and Fe(II) enforce different coordination symmetries. Cu(II)

complexes preferentially adopt tetragonal symmetry, while Fe(II) complexes prefer tetrahedral symmetry.

In addition to the structural information, insight into the function of the metal ion in the quinone acceptor complex can be gained from metal substitution. The case for a direct redox function for the metal is further weakened by these results, thus directing attention to possible ionic functions. In this capacity, it has been difficult to separate the contributions of the protein from those exclusively attributable to the metal.

It should be possible to test whether the charge density of the metal ion directly influences the free energy of Q_A^-/Q_A by examining the redox potential dependence (E_0) in chromatophore membranes biosynthetically substituted with divalent ions of different sizes. Preliminary results on chromatophores that incorporate Cu, Mn, and Zn into the reaction center indicate that there is no dependence on the identity of the metal (Buchanan, Prince, and Dismukes, unpublished results). This suggests that there is no differential influence on E_0 for divalent metal ions differing in size or electron occupancy. This does not yet exclude a direct influence of the metal ion on E_0, since no "metal-free" chromatophores exist to test the idea. In metal-extracted reaction centers the redox properties of Q_A are severely altered; it becomes a two-electron acceptor (Debus et al., 1986).

The cumulative results appear to point toward an influence of the quinone environment (protein and metal) in kinetically stabilizing the states $P^+Q_A^-$ and $P^+Q_B^-$ against wasteful recombination. Two earlier proposals remain possible: conformational relaxation of the reaction center around the charge transfer state, thereby increasing the equilibrium distance of separation P^+ and Q^- (Kleinfeld et al., 1984), or localization of the electron on the semiquinone by vibronic trapping of the initial π anion radical of Q_A^- to form the H-bonded, oxygen-centered radical $ImH_A\cdots QH^\bullet$ (Ferris et al., 1983). In both models it is the repopulation of the nascent (unrelaxed) charge-transfer state that determines the rate of recombination. This latter interpretation has received recent support on the basis of electronic structure calculations, which also showed that the metal may serve to promote direct electron transfer through the imidazoles that are H-bonded to Q_A and Q_B (Buchanan et al., 1986).

ACKNOWLEDGMENTS

We thank Dr. David Kleinfeld for discussions on several occasions, Dr. F. Reiss-Husson for the donation of bacterial cell cultures, Drs. Sandra Eaton and Gareth Eaton for the provision of computer-simulated EPR spectra, and Dr. S. J. Lippard for unpublished EPR data.

Registry No. Cu, 7440-50-8.

REFERENCES

Abragam, A., & Bleany, B. (1970) in *Electron Paramagnetic Resonance of Transition Ions*, p 31, Oxford University Press, London.

Agalidis, I., & Reiss-Husson, F. (1983) *Biochim. Biophys. Acta 724*, 340.

Aktar, F., Goodgame, D. M. L., Goodgame, M., Rayner-Canham, G. W., & Skaps, A. C. (1968) *Chem. Commun.*, 1389.

Boas, J. F., Pilbrow, J. R., & Smith, T. D. (1978) in *Biological Magnetic Resonance* (Berliner, L. T., & Reuben, J., Eds.) Vol. 1, Chapter 7, p 277, Plenum, New York.

Boso, B., Debrunner, P., Okamura, M. Y., & Feher, G. (1981) *Biochim. Biophys. Acta 638*, 173.

Buchanan, S. K., Ferris, K., & Dismukes, G. C. (1986) in *Progress in Photosynthetic Research* (Biggins, J., Ed.) Vol. 1, Chapter 4, pp 193–196, Martinus-Nijhoff, Amsterdam.

Butler, W. F., Johnson, D. C., Shore, H. B., Fredkin, D. R., Okamura, M. Y., & Feher, G. (1980) *Biophys. J. 32*, 967.

Butler, W. F., Calvo, R., Fredkin, D. R., Isaacson, R. A., Okamura, M. Y., & Feher, G. (1984) *Biophys. J. 45*, 947.

Davis, W. M., Zask, A., Nakanishi, K., & Lippard, S. J. (1985) *Inorg. Chem. 24*, 3737.

Debus, R. J., Feher, G., & Okamura, M. Y. (1985a) *Biochemistry 24*, 2488.

Debus, R. J., Okamura, M. Y., & Feher, G. (1985b) *Biophys. J. 47*, 3a.

Debus, R. J., Feher, G., & Okamura, M. Y. (1986) *Biochemistry 25*, 2276.

Deisenhofer, J., Epp, O., Miki, K., Huber, R., & Michel, H. (1984) *J. Mol. Biol. 180*, 385.

Deisenhofer, J., Epp, O., Miki, K., Huber, R., & Michel, H. (1985) *Nature (London) 318*, 618.

Dismukes, G. C., & Siderer, Y. (1981) *Proc. Natl. Acad. Sci. U.S.A. 78*, 274.

Dismukes, G. C., Frank, H. A., Friesner, R., & Sauer, K. (1979) *Biophys. J. 25*, 54a.

Dismukes, G. C., Frank, H. A., Friesner, R., & Sauer, K. (1984) *Biochim. Biophys. Acta 764*, 253.

Dutton, P. L., Leigh, J. S., & Reed, D. W. (1973) *Biochim. Biophys. Acta 292*, 654.

Dutton, P. L., Prince, R. C., & Tiede, D. M. (1978) *Photochem. Photobiol 28*, 939.

Falk, K., Ivanova, E., Roos, B., & Vanngard, T. (1970) *Inorg. Chem. 9*, 556.

Feher, G., & Okamura, M. Y. (1978) in *The Photosynthetic Bacteria* (Clayton, R. K., & Sistrom, W. R., Eds.) pp 349–386, Plenum, New York.

Feher, G., Okamura, M. Y., & McElroy, J. D. (1972) *Biochim. Biophys. Acta 267*, 222.

Feher, G., Isaacson, R. A., McElroy, J. D., Ackerson, L. C., & Okamura, M. Y. (1974) *Biochim. Biophys. Acta 368*, 135.

Feher, G., Isaacson, R. A., Debus, R. J., & Okamura, M. Y. (1986) *Biophys. J. 49*, 585a.

Ferris, K. F., Petrouleas, V., & Dismukes, G. C. (1983) *Abstracts of Papers*, 186th National Meeting of the American Chemical Society, INOR, p 364, American Chemical Society, Washington, DC.

Fransson, G., & Lundberg, B. K. S. (1972) *Acta Chem. Scand. 26*, 3969.

Gunner, M. R., Dutton, P. L., Woodbury, N. W., & Parson, W. W. (1986) *Biophys. J. 49*, 586a.

Guzy, C. M., Raynor, J. B., & Symons, M. C. R. (1969) *J. Chem. Soc. A*, 2299.

Hathaway, B. J., & Billing, D. E. (1970) *Coord. Chem. Rev. 5*, 143.

Imhoff, J. F., Truper, H. G., & Pfenning, N. (1984) *Int. J. Syst. Bacteriol. 34*, 340.

Jolchine, G., & Reiss-Husson, F. (1974) *FEBS Lett. 40*, 5.

Kleinfeld, D., Okamura, M. Y., & Feher, G. (1984) *Biochemistry 23*, 5780.

Michel, H., Epp, O., & Deisenhofer, J. (1986) *EMBO J. 5*, 2445.

Morton, R. A. (1965) in *Biochemistry of Quinones* (Morton, R. A., Ed.) pp 1–21, Academic, New York.

Nam, H. K., Austin, R. A., & Dismukes, G. C. (1984) *Biochim. Biophys. Acta 765*, 301.

Nonaka, Y., Tokii, T., & Kida, S. (1974) *Bull. Chem. Soc. Jpn. 47*, 312.

Okamura, M. Y., Isaacson, R. A., & Feher, G. (1978) *Biophys. J. 21*, 8a.
Parson, W. W., & Cogdell, R. (1975) *Biochim. Biophys. Acta 416*, 105.
Petrouleas, V., & Diner, B. A. (1986) *Biochim. Biophys. Acta 849*, 264.
Petrouleas, V., & Diner, B. A. (1987) *Biochim. Biophys. Acta* (in press).
Pilbrow, J. R. (1969) *Mol. Phys. 16*, 307.
Rakbit, G., Antholine, W. E., Froncizsz, W., Hyde, J. S., Pilbrow, J. R., Sinclair, G. R., & Sartar, B. (1985) *J. Inorg. Biochem. 25*, 217.
Reed, D. W., & Clayton, R. K. (1968) *Biochem. Biophys. Res. Commun. 30*, 471.
Rist, G. H., & Hyde, J. S. (1970) *J. Chem. Phys. 52*, 4633.
Rutherford, A. W., & Evans, M. C. W. (1979) *FEBS Lett. 104*, 227.
Rutherford, A. W., Agalidis, I., & Reiss-Husson, F. (1985) *FEBS Lett. 182*, 151.
Symons, M. R. (1978) in *Chemical and Biochemical Aspects of Electron Spin Resonance Spectroscopy*, pp 136–148, Wiley, New York.
Toy, A. D., Chaston, S. H. H., Pilbrow, J. R., & Smith, T. D. (1971) *Inorg. Chem. 10*, 2219.
VanCamp, H. L., Sands, R. H., & Fee, J. A. (1981) *J. Chem. Phys. 75*, 2098.
Vanngard, T. (1972) in *Biological Applications of Electron Spin Resonance* (Swartz, H. M., Bolton, J. R., & Borg, D. C., Eds.) p 709, Wiley Interscience, New York.
VanWilligan, H., & Chandrashekar, K. T. (1986) *J. Am. Chem. Soc. 108*, 709.
Weast, W. R. (1982) *Handbook of Chemistry and Physics*, 63rd ed., CRC Press, Boca Raton, FL.
Wraight, C. A. (1978) *FEBS Lett. 93*, 283.

Isolation and Characterization of a Subunit Form of the Light-Harvesting Complex of *Rhodospirillum rubrum*†

J. F. Miller, S. B. Hinchigeri, P. S. Parkes-Loach, P. M. Callahan,‡ J. R. Sprinkle, J. R. Riccobono, and P. A. Loach*

Department of Biochemistry, Molecular Biology, and Cell Biology, Northwestern University, Evanston, Illinois 60201

Received December 3, 1986; Revised Manuscript Received April 7, 1987

ABSTRACT: A new method is described for the isolation of subunits of the light-harvesting complex from *Rhodospirillum rubrum* (wild type and the G-9 mutant) in yields that approach 100%. The procedure involved treating membrane vesicles with ethylenediaminetetraacetic acid–Triton X-100 to remove components other than the light-harvesting complex and reaction center. In the preparation from wild-type cells, a benzene extraction was then employed to remove carotenoid and ubiquinone. The next step involved a careful addition of the detergent *n*-octyl β-D-glucopyranoside, which resulted in a quantitative shift of the long-wavelength absorbance maximum from 873 to 820 nm. This latter complex was then separated from reaction centers by gel filtration on Sephadex G-100. The pigment–protein complex, now absorbing at 820 nm, contained two polypeptides of about 6-kilodalton molecular mass (referred to as α and β) in a 1:1 ratio and two molecules of bacteriochlorophyll (BChl) for each αβ pair. This complex is much smaller in size than the original complex absorbing at 873 nm but probably is an associated form such as $\alpha_2\beta_2$·4BChl or $\alpha_3\beta_3$·6BChl. The 820-nm form could be completely shifted back to a form once again having a longer wavelength λ_{max} near 873 nm by decreasing the octyl glucoside concentration. Thus, the complex absorbing at 820 nm appears to be a subunit form of the original 873-nm complex.

In recent years, considerable progress has been made in isolating light-harvesting (LH)[1] complexes from photosynthetic organisms (Thornber, 1986; Drews, 1985; Zuber, 1985, 1986; Cogdell, 1986; Gantt, 1986; Anderson & Barrett, 1986; Michel-Beyerle, 1985). Many of these preparations were sufficiently pure that the polypeptide components of the complexes have been well characterized including the determination of their amino acid sequences (Brunisholz et al., 1981, 1984, 1985; Gogel et al., 1983; Tadros et al., 1983, 1985; Theiler et al., 1984a,b, 1985; Wechsler et al., 1985). In addition, the genes coding for the protein of such complexes have been isolated, cloned, and sequenced (Youvan et al., 1984; Coruzzi, et al., 1983; Fish et al., 1985). However, because of the inherent instability of chlorophyll and bacterio-

† This research was supported by research grants from the U.S. Public Health Service (GM 11741) and the National Science Foundation (PCM-7816669).

* Address correspondence to this author.
‡ Present address: Department of Chemistry, University of Nebraska—Lincoln, Lincoln, NE 68588-0304.

[1] Abbreviations: BChl, bacteriochlorophyll; B881, the core light-harvesting complex of wild-type *R. rubrum* whose long-wavelength absorbance maximum is at 881 nm; B873, the core light-harvesting complex of the G-9 mutant (carotenoidless) of *R. rubrum* or the wild-type light-harvesting complex after benzene extraction (also now absorbing at 873 nm); B820, the subunit form of B873 now absorbing at 820 nm after treatment with octyl glucoside; "B873", the reassociated form of B820 whose absorbance band is near 873 nm; B873-α, the polypeptide of B873 soluble in 1:1 $CHCl_3$–CH_3OH and running larger (slower) than the β-polypeptide on SDS–PAGE; B873-β, the other polypeptide of B873 which runs smaller (faster) on SDS–PAGE and does not dissolve in 1:1 $CHCl_3$–CH_3OH; LH, light harvesting; OG, *n*-octyl β-D-glucopyranoside; RC, reaction center; SDS–PAGE, sodium dodecyl sulfate–polyacrylamide gel electrophoresis; kDa, kilodalton(s); EDTA, ethylenediaminetetraacetic acid; HPLC, high-performance liquid chromatography; Tris, tris(hydroxymethyl)aminomethane; PTC, phenylthiocarbamyl; OPA, *o*-phthalaldehyde; cmc, critical micelle concentration; CD, circular dichroism; LDAO, lauryldimethylamine *N*-oxide; BPh, bacteriopheophytin.

0006-2960/87/0426-5055$01.50/0